Nuclear quantum effects on electron transfer reactions in DNA hairpins

Shigenori Tanaka*
Advanced Materials & Devices Laboratory, Corporate R & D Center, Toshiba Corporation, Kawasaki 212-8582, Japan

Yasuo Sengoku
Department of Knowledge-Based Information Engineering, Toyohashi University of Technology, Toyohashi 441-8580, Japan

(Received 29 October 2002; published 11 September 2003)

The driving force dependence of photoinduced electron transfer rate constant in synthetic DNA hairpins in aqueous solutions has been analyzed by means of molecular dynamics simulations. The quantum energy gap law has thus been investigated from a fully atomistic point of view, well reproducing the experimental results with reduced ambiguities in the parameter fitting. Although the contribution from the high-frequency vibrational modes of DNA and water solvent to the reorganization energy is fairly small, their quantum effect on the electron transfer rate constant is significant, well accounting for the deviation from the Marcus parabola observed in the experiments.

DOI: 10.1103/PhysRevE.68.031905 PACS number(s): 87.14.Gg, 87.15.Aa, 72.80.Le

The charge transfer reactions in DNA have recently attracted much attention in the contexts of biological interests such as radiation-induced damage and repair of genes [1] and of nanotechnology applications using DNA duplexes as molecular wires [2]. Considerable experimental and theoretical efforts have focused on the elucidation of long-range electron transfer (ET) in DNA where the ET rate constant is usually expressed as [3–5]

$$k = k_0 \exp(-\beta r) \tag{1}$$

as a function of the distance r between the donor and the acceptor with a decay constant β. This exponential dependence may essentially be considered to be of electronic origin, and there have been many debates concerning this issue [4]. Recent advances in the investigations [2] have then led to a finding of an important role played by the guanine (G) base as a hole trap because it has a lower ionization potential compared to the other bases, adenine (A), cytosine (C), and thymine (T).

As has been elucidated by the standard theories for ET reactions [3,5], the rate constant is also controlled by the structural relaxation effects of molecules surrounding the donor, acceptor, and mediators of ET. Such an effect is compactly expressed in terms of the donor-acceptor free-energy gap ΔG and the reorganization energy λ in the nuclear Franck-Condon factor. Recently, an intriguing experiment by Lewis *et al.* [6] focusing on a systematic elucidation of this effect has appeared, in which the photoinduced charge transfer rate constant in DNA hairpins in aqueous solution has been measured as a function of energy gap ΔG by varying the species of linker chromophores such as stilbene (see Fig. 1). They measured both charge-separation (CS) and charge recombination (CR) reactions between the linker chromophore (electron acceptor) and the G base (electron donor or hole acceptor) by means of time-resolved transient absorption spectroscopy, and explained the experimental data in terms of the semiclassical Marcus-Levich-Jortner formula [3,5]. They then found that the CS and CR reactions belong to the normal and inverted regions of ET, respectively, and that a nuclear quantum effect, represented by a single high-frequency (1500 cm^{-1}) mode, plays a considerable role. It may be pointed out, however, that there is an ambiguity in the discrimination between the low-frequency (classical) solvent modes and the high-frequency (quantum) modes in the parameter fitting based on the semiclassical model, and that other high-frequency modes such as those associated with the stretching modes of water molecules with frequency exceeding 3000 cm^{-1} exist. The major purpose of the present work is therefore to attempt a more quantitative theoretical analysis on the experiment [6] from a fully atomistic point of view relying on molecular dynamics (MD) simulations and the quantum theory for ET.

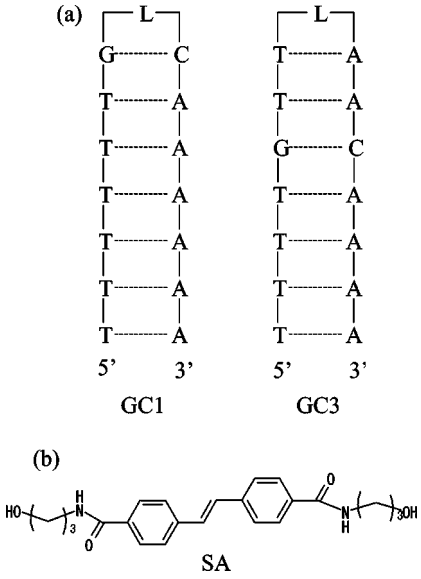

FIG. 1. (a) Structures of DNA hairpins with nearest-neighbor (GC1) and bridge-mediated (GC3) nucleobase quenchers. (b) Structure of linker (L) chromophore, SA.

*Electronic address: tanaka2@arl.rdc.toshiba.co.jp

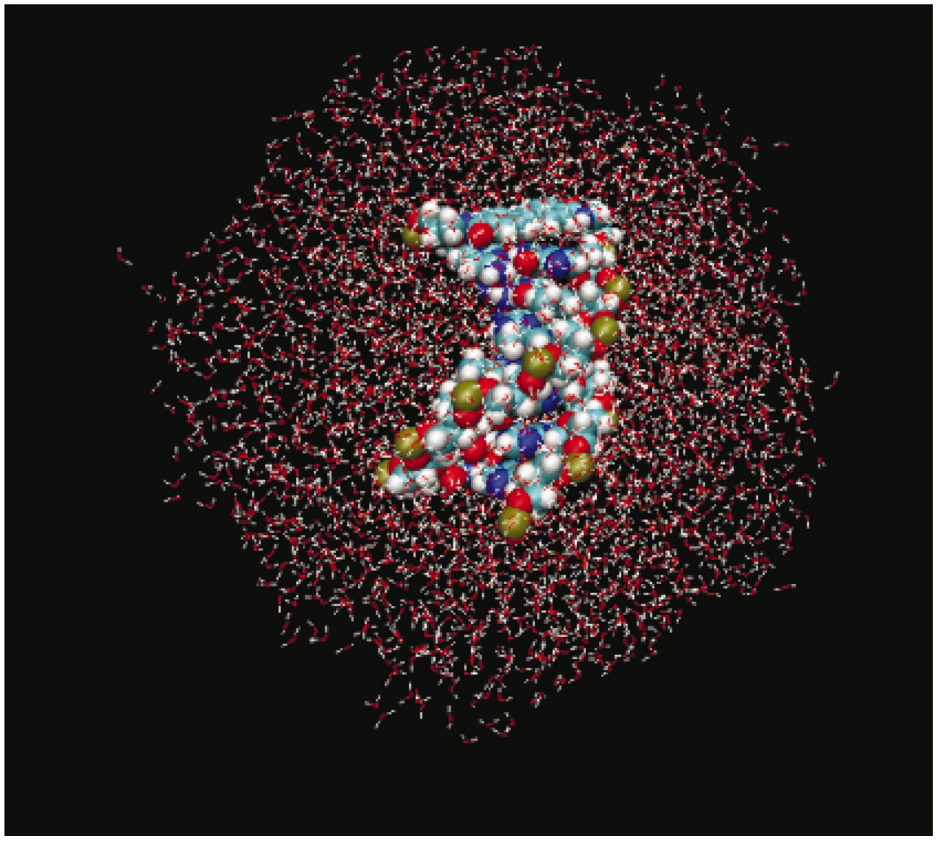

FIG. 2. (Color) Snapshot of the MD run for the GC1 with the neutral SA in the ground state surrounded by a water-solvent sphere.

The ET rate constant between the linker chromophore and the G base is given by [7–10]

$$k=\frac{V^2}{\hbar^2}\mathrm{Re}\left(\int_{-\infty}^{\infty}dt\,\exp[F(t)]\right) \tag{2}$$

in the nonadiabatic limit. Here V refers to the electronic coupling constant and

$$F(t)=\frac{i}{\hbar}\Delta G t+\frac{2}{\pi\hbar}\int_0^{\infty}d\omega\frac{J(\omega)}{\omega^2}\times\left[(\cos\omega t-1)\coth\left(\frac{\hbar\omega}{2k_{\mathrm{B}}T}\right)+i\sin\omega t\right], \tag{3}$$

with the Boltzmann constant k_{B} and the Planck constant $\hbar$. This function describing the nuclear Franck-Condon factor is thus governed by the donor-acceptor energy gap ΔG and the spectral density $J(\omega)$ associated with the surrounding structural fluctuations. The spectral density can then be calculated through MD simulations. Let us consider the reaction coordinate for ET as

$$\Delta V=H_i-H_f, \tag{4}$$

where H_i and H_f are the (electronically) diabatic nuclear Hamiltonians in the initial and final states of ET. We then consider the fluctuation around the thermal average

$$\delta\Delta V(t)=\Delta V(t)-\langle\Delta V(t)\rangle \tag{5}$$

and its time correlation function (TCF) as

$$\langle\delta\Delta V(0)\,\delta\Delta V(t)\rangle=\frac{4k_{\mathrm{B}}T}{\pi}\int_0^{\infty}d\omega\frac{J(\omega)}{\omega}\cos\omega t, \tag{6}$$

which is related to the Fourier transform of the spectral density at temperature T. The classical limit ($\hbar\to 0$) of Eq. (2) is the Marcus formula [3]

$$k=\frac{2\pi}{\hbar}V^2\left(\frac{1}{4\pi\lambda k_{\mathrm{B}}T}\right)^{1/2}\exp\left[-\frac{(\Delta G+\lambda)^2}{4\lambda k_{\mathrm{B}}T}\right], \tag{7}$$

where the reorganization energy is given by

$$\lambda=\frac{2}{\pi}\int_0^{\infty}d\omega\frac{J(\omega)}{\omega}. \tag{8}$$

We carried out the MD simulations for the DNA hairpins in water with the TINKER [11] package. As for the force field, we used the AMBER [12] for the DNA hairpins and the flexible TIP3P [13,14] for the surrounding water molecules. In order to accelerate the calculations for nonbonded interactions such as the Coulombic and van der Waals forces, the MD Engine II (Fuji Xerox Co., Ltd., see Ref. [30]) was employed for the parallel computing without the long-range cutoff. Concerning the structures of DNA hairpins, we have considered those studied by Lewis *et al.* [6], one (GC1) in which the GC pair is adjacent to the stilbene-4, 4′-dicarboxamide (SA) linker and another (GC3) in which the GC pair is separated from the SA linker by two intervening TA pairs, as shown in Fig. 1. The initial structures of the

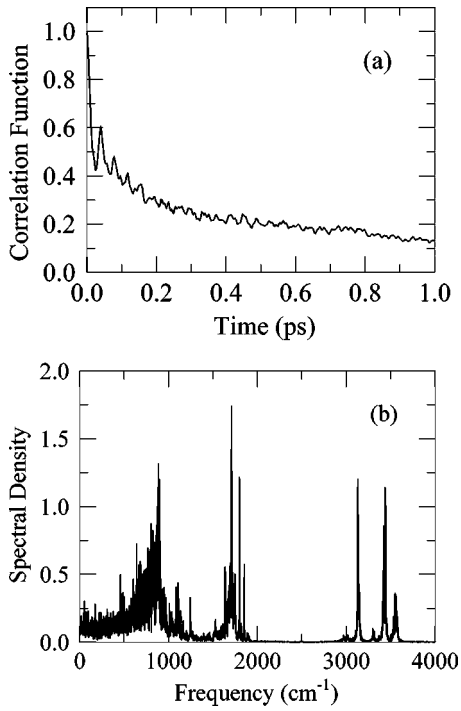

FIG. 3. (a) The normalized TCF $C(t)$ and (b) the normalized spectral density $\tilde{J}(\omega)$ for the GC1 with the neutral SA in the ground state.

B-form DNA hairpins together with 16 Na^+ counterions were generated with the HyperChem (Release 6.02, Hypercube, Inc., Gainesville, FL, 1999) package and then embedded in a water sphere with a radius of 30 Å. For the neutral and charge-separated states of SA linker and G base, we performed the molecular orbital calculations and the structural optimizations with the Hatree-Fock/6-31G* method using the GAUSSIAN 98 [15] package. The atomic charge distributions for them were then calculated with the aid of the restrained electrostatic potential method [16]. Regarding the neutral state of the SA linker with which the MD runs were performed, we carried out the calculations both for the (electronically) ground and excited states using the configuration-interaction-singles method [15] for the latter. After the structural optimizations for the DNA hairpins and the surrounding water molecules requiring the gradient norm less than 1.0 kcal/mol/Å, the isothermal MD simulations at $T=300$ K were performed for 150 ps, in which, after the equilibration, the last 100-ps data were used for the calculations of the TCF and the spectral density. The snapshot for an MD run is shown in Fig. 2.

The calculated results for the normalized TCF

$$C(t)=\langle \delta\Delta V(0)\delta\Delta V(t)\rangle/\langle \delta\Delta V(0)^2\rangle \tag{9}$$

and the normalized spectral density

$$\tilde{J}(\omega)=J(\omega)\Big/\int_0^\infty d\omega\frac{J(\omega)}{\omega} \tag{10}$$

are shown in Figs. 3(a) and 3(b), respectively, for the GC1. In Fig. 3(a) we can see typical oscillations associated with

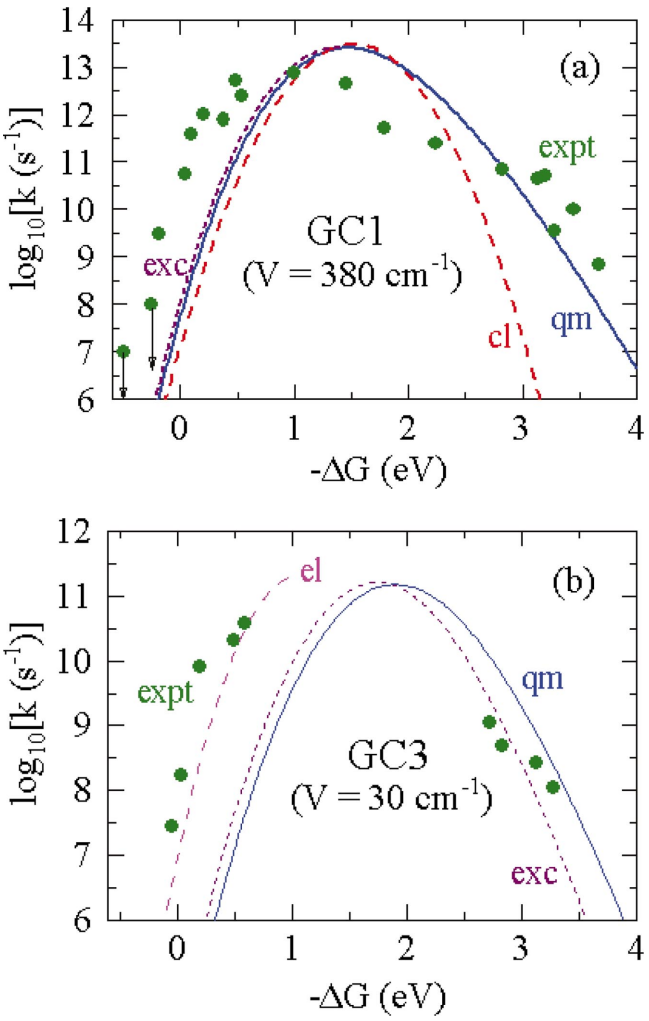

FIG. 4. (Color) The free-energy dependence of the ET rate constant for (a) GC1 and (b) GC3 hairpins. Blue solid line (qm): quantum-mechanical result with the SA in the ground state. Red dashed line (cl): classical result with the SA in the ground state. Purple dotted line (exc): quantum-mechanical result with the SA in the excited state. Pink dashed line (el): quantum-mechanical result with the SA in the excited state, where the optical dielectric constant $\epsilon_\infty=1.79$ was employed. Green solid circles (expt): experimental results [6].

the intramolecular and intermolecular motions. Roughly speaking, the contributions to the spectral density in Fig. 3(b) stem from the three frequency regimes: that from the regime below about 1000 cm^{-1} mainly refers to the contribution associated with the diffusive modes of translational, rotational, and librational motions of water solvent, which includes the Debye relaxation region [8,17,18]; that between 1500 and 2000 cm^{-1} mainly corresponds to the intramolecular bending modes of water molecules; and that above 3000 cm^{-1} may be assigned for the stretching modes of water molecules. It should be remarked, however, that the contributions from the DNA hairpins are superimposed on those from the water solvent, giving a more complicated spectrum compared to that for the latter alone. For example, the peak at around 3100 cm^{-1} refers to the contribution from the stretching modes of hydrogen atoms contained in the DNA

hairpin. We can then calculate the electron transfer rate constant k as a function of the energy gap ΔG on the basis of Eq. (2). Here we assume that the spectral density $J(\omega)$ and the electronic coupling constant V are virtually identical among each series of all the GC1- or GC3-type molecular structures investigated in the experiments [6] irrespective of the species of the linker chromophores. The calculated results for k are depicted in Fig. 4.

The position of the maximum in the $-\Delta G$ versus k curve is essentially given at $-\Delta G=\lambda$, as indicated in Eq. (7), distinguishing the normal region ($-\Delta G<\lambda$) from the inverted region ($-\Delta G>\lambda$) [3]. Taking into account the contributions from the electronic polarization, we have renormalized the reorganization energy λ' by a scaling factor as [19]

$$\lambda'/\lambda=\left(\frac{1}{\epsilon_\infty}-\frac{1}{\epsilon_0}\right)\Big/\left(1-\frac{1}{\epsilon_0}\right), \tag{11}$$

using the static (ϵ_0) and optical (ϵ_∞) dielectric constants. The quantum-mechanical result, ''qm,'' in Fig. 4(a) has thus been calculated employing $\epsilon_0=78.4$ [20] and $\epsilon_\infty=1.111$ [21] for the GC1 with the neutral SA in the ground state. The corresponding classical limit, ''cl,'' and the result for the SA in the excited state, ''exc,'' are also depicted in the same figure [22] in comparison with the experimental values [6], ''expt,'' denoted by the solid circles. It is observed in the figure that the quantum-mechanical calculation can satisfactorily reproduce the experimental results [6] without resorting to intentional parameter fittings except for the magnitude of the (unknown) electronic coupling constant V, which is estimated to be 380 cm^{-1} in the case of GC1. Remarks are also in order regarding the significant difference between the classical and quantum calculations for k in the inverted region by as much as a factor of 10^3 or more at around $-\Delta G=3$ eV, which markedly represents an important role played by the nuclear quantum effects primarily associated with hydrogen atoms, and is actually observed in the experiments [6].

We observe in Fig. 4 that discrepancies still remain between calculation and experiment. Possible origins for them include the following. First, the value for the electronic coupling constant V is fixed in the calculation, neglecting the variations in V according to the species of linker chromophores. Second, there may be doubts regarding the accuracy of the AMBER force field [12] for the calculation of the reorganization energy, especially in the case of GC3, where the long-range structural fluctuations in the DNA duplex may be emphasized more significantly. Third, there is an ambiguity in the reorganization energy arising from the contributions of the electronic polarization, as shown in Eq. (11); we obtain the curve denoted as ''el'' in Fig. 4(b) if we use $\epsilon_\infty=1.79$ [23] instead of 1.111 in the case of GC3 with the SA in the excited state. Fourth, some mixing of incoherent hopping processes [2] into the coherent one-step electron transfer presumed in the present model may cause some errors, especially in the case of GC3. Fifth, there may be uncertainties in the experimental estimates [6,24] for the value of ΔG, causing a shift in the ΔG-k curve. Finally, the harmonic, nonadiabatic, and Condon approximations underlying the theoretical analysis [7–10] may bring about some errors such as those associated with the fluctuating effective electronic coupling [25].

TABLE I. Decomposition of the reorganization energy λ' into the components in specific frequency ranges based on Eqs. (8) and (11) in the case of GC1 with SA in the ground state.

Frequency range (cm^{-1})	Partial λ' (eV)	(%)
0–800	1.257	83.0
800–1400	0.172	11.4
1400–2500	0.059	3.9
2500–4000	0.026	1.7

In conclusion, we have performed MD simulations for explaining the driving force dependence of ET rate constant in DNA hairpins in aqueous solutions and succeeded in well reproducing the experimental results [6] with minimal parameter fitting. The primary adjustable parameter, which could be obtained through the molecular orbital calculations, is the (effective) electronic coupling constant whose optimal value has been estimated to be $V=380$ and 30 cm^{-1} for GC1 and GC3, respectively, giving a reasonable value for the electronic decay constant of $\beta=0.75$ $\mathrm{Å}^{-1}$ in Eq. (1). An additional uncertainty may also come from the contributions of the electronic polarization. We have then identified significant nuclear quantum effects in the inverted region of the ΔG-k curve through comparison with the experimental results. It should also be remarked, however, that the contributions from the high-frequency modes to the reorganization energy, which includes both the inner and outer sphere parts [3], are relatively small, as shown in Table I. Thus, although the total value of $\lambda'=1.51$ eV in the GC1 agrees fairly well with the value of 1.22 eV estimated by Lewis *et al.* [6], the decomposition into the constituents seems quite different. In the latter analysis the total reorganization energy was decomposed into a sum of the contributions from the low-frequency solvent mode ($\lambda_s=0.23$ eV) and the high-frequency (1500 cm^{-1}) quantum mode ($\lambda_i=0.99$ eV), whereas the present analysis has found that the reorganization energy associated with the low-frequency modes is overwhelmingly dominant, which is consistent with other theoretical estimates [26–29] based on the dielectric model.

We would like to thank A. Okada, N. Kurita, and O. Okada for useful discussions. Technical assistance by Y. Kumagai on the numerical calculations is also appreciated. This work was supported by Research and Development for Applying Advanced Computational Science and Technology of Japan Science and Technology Corporation (ACT-JST).

[1] D.T. Odom and J.K. Barton, Biochemistry **40**, 8727 (2001).
[2] C. Dekker and M.A. Ratner, Phys. World **14**(8), 29 (2001).
[3] R.A. Marcus and N. Sutin, Biochim. Biophys. Acta **811**, 265 (1985).
[4] D.N. Beratan, S. Priyadarshy, and S.M. Risser, Chem. Biol. **4**, 3 (1997).
[5] M. Bixon and J. Jortner, Adv. Chem. Phys. **106**, 35 (1999).
[6] F.D. Lewis, R.S. Kalgutkar, Y. Wu, X. Liu, J. Liu, R.T. Hayes, S.E. Miller, and M.R. Wasielewski, J. Am. Chem. Soc. **122**, 12 346 (2000).
[7] J.S. Bader, R.A. Kuharski, and D. Chandler, J. Chem. Phys. **93**, 230 (1990).
[8] X. Song and R.A. Marcus, J. Chem. Phys. **99**, 7768 (1993).
[9] K. Ando, J. Chem. Phys. **106**, 116 (1997).
[10] S. Tanaka and C.-P. Hsu, J. Chem. Phys. **111**, 11 117 (1999).
[11] M.J. Dudek and J.W. Ponder, J. Comput. Chem. **16**, 791 (1995).
[12] W.D. Cornell, P. Cieplak, C.I. Bayly, I.R. Gould, K.M. Merz, Jr., D.M. Ferguson, D.C. Spellmeyer, T. Fox, J.W. Caldwell, and P.A. Kollman, J. Am. Chem. Soc. **117**, 5179 (1995).
[13] W.L. Jorgensen, J. Chandrasekhar, J. Madura, R.W. Impey, and M.L. Klein, J. Chem. Phys. **79**, 926 (1983).
[14] L.X. Dang and B.M. Pettitt, J. Phys. Chem. **91**, 3349 (1987).
[15] M.J. Frisch *et al.*, computer code GAUSSIAN 98, Revision A.1 (Gaussian, Inc., Pittsburgh, PA, 1998).
[16] C.I. Bayly, P. Cieplak, W.D. Cornell, and P.A. Kollman, J. Phys. Chem. **97**, 10 269 (1993).
[17] M. Neumann, J. Chem. Phys. **85**, 1567 (1986).
[18] In the very low-frequency regime (say, $<20\ \mathrm{cm}^{-1}$), the calculated spectral densities show an approximately linear dependence on the frequency with large statistical fluctuations.
[19] K. Ando, J. Chem. Phys. **114**, 9470 (2001).
[20] We have employed the static dielectric constant for the water solvent in spite of the fact that this could not be applied to the DNA parts. This is because the contribution to the spectral density arising from the water solvent is overwhelmingly dominant, as seen through the comparison with the results accounting only for the water solvent [9].
[21] K. Ando, J. Chem. Phys. **115**, 5228 (2001).
[22] As for the neutral state of SA, the charge distributions in the excited and ground states should be used for the CS and CR processes, respectively.
[23] A.D. Buckingham, Proc. R. Soc. London, Ser. A **238**, 235 (1956).
[24] S. Steenken and S.V. Jovanovic, J. Am. Chem. Soc. **119**, 617 (1997).
[25] A. Troisi and G. Orlandi, J. Phys. Chem. B **106**, 2093 (2002).
[26] H.L. Tavernier and M.D. Fayer, J. Phys. Chem. B **104**, 11 541 (2000).
[27] G.S.M. Tong, I.V. Kurnikov, and D.N. Beratan, J. Phys. Chem. B **106**, 2381 (2002).
[28] D.M. Basko and E.M. Conwell, Phys. Rev. Lett. **88**, 098102 (2002).
[29] K. Siriwong, A.A. Voityuk, M.D. Newton, and N. Rösch, J. Phys. Chem. B **107**, 2595 (2003).
[30] See http://www.fujixerox.co.jp/nbc/esradd/MDEngineII/indexe.html